# Multiple dielectric loaded perforated screens as frequency selective surfaces

# Multiple dielectric loaded perforated screens as frequency selective surfaces

R. Orta
R. Tascone
R. Zich

*Indexing term: Antennas (reflectors)*

**Abstract:** Perforated screens can be used as frequency selective surfaces when a high pass frequency response is required. In this paper, a spectral characterisation of perforated screens is presented. The analysis yields the generalised scattering matrix of each screen, which is a useful tool for studying composite structures. Numerical results, relative to single and double screens with periodical distributions of circular apertures, are discussed.

## 1 Introduction

Modern reflector antenna systems make use of frequency selective surfaces (FSSs) as free-space diplexers. Two classes of FSS exist: one class has the form of a periodic distribution of conducting patches, sandwiched between dielectric support structures, and has a low pass frequency response, the other class consists of a periodically perforated metallic screen, and has a dual frequency behaviour.

Approximate analyses of these structures have appeared in the literature [1–4], but a complete characterisation can be obtained only through the solution of a boundary value problem. In principle, either the current induced on the conductors, or the aperture electric field can be assumed as the unknown of the problem. Generally, FSSs of the first class are more easily studied using the induced current approach [5–10], while the converse is true for FSSs of the second class [11–13]. However, in some cases, perforated screens have been studied by the induced current approach [14]. The choice of the approach depends essentially on the availability of a convenient set of basis functions to expand the unknown. In this paper, we apply the aperture approach to the analysis of high pass structures, consisting of periodically perforated metallic screens embedded in a stratified dielectric medium.

The problem of the scattering from isolated screens has been addressed by several authors in the past [11–13]. Free-standing double screen structures have been studied by the mutual impedance method [15]. The effect of dielectrics was first taken into account in Reference 16, by a mode matching analysis in the case of a biplanar slot array in a symmetrical configuration. An alternative approach to the scattering analysis of free-standing double arrays, based on a system of coupled integral equations was proposed in Reference [17]. These methods are not satisfactory since the formulation must be modified in the case of more complex structures (nonsymmetrical configurations or more than two arrays). A better procedure consists in characterising each array with a well defined standard loading, as it is implicit in the definition of the scattering matrix. In this way, the analysis of a multiple grid structure is reduced to the cascading of a number of $N$-port blocks by circuit techniques. According to this approach, one can define the free-standing grids and the dielectric layers separately as blocks, using the free-space Green function for the characterisation of each grid [18]. However, in this way, the cascading procedure is computationally inefficient when the grids are etched on a dielectric support, because it requires the inversion of large matrices, with size equal to the number of Floquet modes used for the characterisation of the grids. To increase the efficiency, that is, to reduce the size of the matrices to be inverted, one must consider the presence of the dielectric layers directly in the characterisation of each grid. A step in this direction was taken by Johansson [19], but he considered each grid with a dielectric layer on one side only as a block.

Our effort has been to develop a general formulation, based on the transmission line technique [20], which leads to the definition of the generalised scattering matrix (GSM) of elementary blocks, constituted by each grid with its embedding dielectric layers. The presence of the dielectrics on both sides of the grid is taken directly into account in the definition of the relevant Green function. In this way, the number of ports to be connected is greatly reduced, since only the lowest order Floquet modes take part effectively in the interaction between the grids.

## 2 Formulation

Let us consider a metallic screen, with an arbitrary distribution of apertures, covered on both sides with a stratified dielectric medium (see Fig. 1). The case of a periodic arrangement of identical apertures will be treated as a special case of the general formulation. This kind of structure can be seen as a transversal discontinuity in an open waveguide with homogeneous cross section, and the scattering problem can be attacked by modal techniques. As is well known, the mode eigenfunctions are exponentials which constitute a continuous spectrum of plane waves. As a consequence, the modal voltages and currents are the polar components of the Fourier transform of the transverse electric and magnetic fields. This

Paper 5895H (E11), received 9th June 1987

The authors are with CESPA (CNR) and Departmento de Electronica, Politechnico di Torino, Corso Duca Degli Abruzzi 24, 10129 Torino, Italy

implies the possibility of solving the scattering problem directly in the spectral domain using a vector formulation.

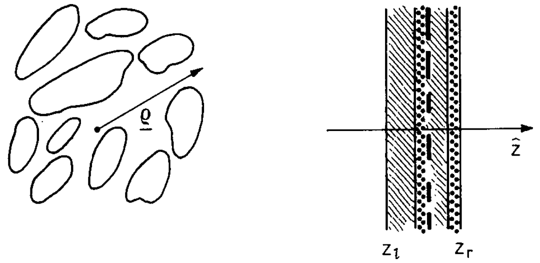


**Fig. 1** *Perforated screen geometry, front and side views*

Assuming an arbitrary field incident from the left side of the structure shown in Fig. 1, we obtain, by the transmission line formalism [20], the equivalent circuit of Fig. 2 relative to a generic value of the spectral variable $\underline{k}$ (conjugate to the transversal coordinate $\underline{\varrho}$).

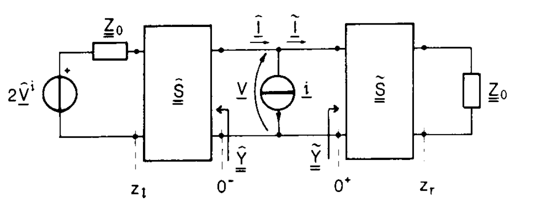


**Fig. 2** *Vector equivalent circuit of the structure of Fig. 1 for a generic free-space mode*

The source is assumed to be on the left hand side. The equivalence theorem is used to substitute the metallic screen with a distribution of electric currents. $\underline{\underline{\hat{S}}}$ and $\underline{\underline{\tilde{S}}}$ are the $2 \times 2$ dyadic scattering matrices of the dielectric layers. $\underline{\underline{Z}}_0$ is the free-space dyadic modal impedance

We have applied the Equivalence Theorem to substitute the metallic screen with an unknown distribution of electric currents $\underline{J}(\underline{\varrho})$. Voltages and currents in this circuit are vector functions of $\underline{k}$ and are the Fourier transforms of the transverse electric ($\underline{E}_t$) and magnetic ($\underline{H}_t \times \hat{z}$) field, respectively. With these definitions, TM and TE modes can be treated simultaneously. Impedances and admittances are dyadic operators and, for example, the modal free-space dyadic impedance is defined as

$$\underline{\underline{Z}}_0(\underline{k}) = \beta/(\omega\varepsilon_0)\,\hat{k}\hat{k} + (\omega\mu_0)/\beta\,(\hat{k} \times \hat{z})(\hat{k} \times \hat{z}) \qquad (1)$$

where

$$\beta = \sqrt{(K_0^2 - |\underline{k}|^2)} \qquad \hat{k} = \underline{k}/|\underline{k}|$$

The voltage generator has strength $2\underline{V}^i$ where $\underline{V}^i(\underline{k})$ is the Fourier transform of the incident electric field at section $z = z_l$. The current generator at section $z = 0$ has strength $\underline{i}(\underline{k})$ equal to the Fourier transform of the sum of the electric currents induced on both sides of the screen $\underline{J}(\underline{\varrho})$. The presence of this current generator is directly connected to the existence of a magnetic field discontinuity at $z = 0$, [20]. The dielectric stratifications on the left and right side of the screen are characterised by their $2 \times 2$ scattering matrices $\underline{\underline{\hat{S}}}(\underline{k})$ and $\underline{\underline{\tilde{S}}}(\underline{k})$, respectively, whose elements are dyadic operators.

Both the total voltage at $z = 0$ $\underline{V}(\underline{k})$ and the impressed current $\underline{i}(\underline{k})$ are unknown, and satisfy the following equation which can be easily obtained from the circuit of Fig. 2:

$$-[\underline{\underline{\hat{Y}}}(\underline{k}) + \underline{\underline{\tilde{Y}}}(\underline{k})]^{-1} \cdot \underline{i}(\underline{k}) + \underline{\underline{\hat{T}}}_t(\underline{k}) \cdot \underline{V}^i(\underline{k}) = \underline{V}(\underline{k}) \qquad (2)$$

$\underline{\underline{\hat{Y}}}(\underline{k})$, $\underline{\underline{\tilde{Y}}}(\underline{k})$ are the load admittances seen by the current generator looking to the left and to the right, respectively. $\underline{\underline{\hat{T}}}_t(\underline{k})$ is a transmission operator linking the incident voltage to the total voltage at section $z = 0$, when the screen is removed. We use the symbols ˆ and ˜ to denote quantities relative to the left and right region with respect to the screen, respectively. Eqn. 2 describes completely the scattering problem, even if it contains two unknowns. This is due to the analytical properties of the two functions $\underline{V}(\underline{k})$ and $\underline{i}(\underline{k})$ that are transforms of functions with complementary supports: $\underline{E}_t(\underline{\varrho})$ vanishes on the conducting surface whereas $\underline{J}(\underline{\varrho})$ vanishes on the apertures. These properties can be exploited to solve the problem directly in the spectral domain by the Galerkin method of moments. Since we want to use the aperture approach, and hence expand $\underline{V}(\underline{k})$ on a set of basis functions, it is convenient to rewrite eqn. 2 in the form:

$$-[\underline{\underline{\hat{Y}}}(\underline{k}) + \underline{\underline{\tilde{Y}}}(\underline{k})] \cdot \underline{V}(\underline{k}) + [\underline{\underline{\hat{Y}}}(\underline{k}) + \underline{\underline{\tilde{Y}}}(\underline{k})] \cdot \underline{\underline{\hat{T}}}_t(\underline{k}) \cdot \underline{V}^i(\underline{k}) = \underline{i}(\underline{k}) \qquad (3)$$

Incidentally, it is interesting to note that this equation can also be derived by using the Equivalence Theorem in a different form. In particular, one can substitute the perforated screen with a solid one on the left and right side, of which two distributions of equivalent magnetic current of value $\underline{E} \times (-\hat{z})$ and $\underline{E} \times \hat{z}$, respectively, are present in place of the apertures. Equivalent electric currents do not radiate any field since they are short circuited by the metal plate, and hence they are disregarded. In this way, one arrives at the equivalent circuit of Fig. 3, constituted by two disconnected parts, because of the presence of the solid metallic plate. However, the strengths of the voltage generators at sections $z = 0^-$ and $z = 0^+$ are identical because the transversal electric field is continuous. From this equivalent circuit we easily obtain the following:

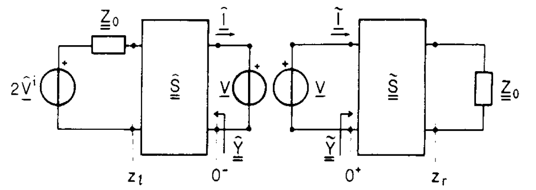


**Fig. 3** *Alternative equivalent circuit of the structure of Fig. 1*

In this case the equivalence theorem is used to substitute the perforated screen with a solid one on which a magnetic current distribution is placed

$$\underline{\hat{I}}(\underline{k}) = \underline{\underline{\hat{Y}}}_t(\underline{k}) \cdot \underline{V}^i(\underline{k}) - \underline{\underline{\hat{Y}}}(\underline{k}) \cdot \underline{V}(\underline{k}) \qquad (4a)$$

$$\underline{\tilde{I}}(\underline{k}) = \underline{\underline{\tilde{Y}}}(\underline{k}) \cdot \underline{V}(\underline{k}) \qquad (4b)$$

where $\underline{\underline{\hat{Y}}}_t(\underline{k})$ is a transadmittance operator linking the incident voltage to the total current at $z = 0$ when the voltage generator $\underline{V}(\underline{k})$ is short-circuited. As previously stated, the function $\underline{i}(\underline{k})$ is the Fourier transform of the transversal magnetic field jump, and hence can be written as follows:

$$\underline{i}(\underline{k}) = \underline{\hat{I}}(\underline{k}) - \underline{\tilde{I}}(\underline{k}) \qquad (5)$$

By substituting eqns. 4*a* and *b* into eqn. 5 we get

$$-[\underline{\underline{\hat{Y}}}(\underline{k}) + \underline{\underline{\tilde{Y}}}(\underline{k})] \cdot \underline{V}(\underline{k}) + \underline{\underline{\hat{Y}}}_t(\underline{k}) \cdot \underline{V}^i(\underline{k}) = \underline{i}(\underline{k}) \qquad (6)$$

which is identical to eqn. 3. In fact, it can be proved by simple circuit considerations that

$$\underline{\underline{\hat{Y}}}_t(\underline{k}) = [\underline{\underline{\hat{Y}}}(\underline{k}) + \underline{\underline{\tilde{Y}}}(\underline{k})] \cdot \underline{\underline{\hat{T}}}_t(\underline{k})$$

To solve eqn. 6 by Galerkin method of moments, we introduce a set of vector basis functions $\{\underline{g}_n(\underline{k})\}$, to expand the Fourier transform of the aperture electric field as follows:

$$\underline{V}(\underline{k}) = \sum_n X_n \underline{g}_n(\underline{k}) \tag{7}$$

Then we equate to zero the projections of the unknown function $\underline{i}(\underline{k})$ given by eqn. 6 on the same set $\{\underline{g}_n(\underline{k})\}$. The problem is now reduced to the solution of a linear system of equations in the unknown coefficients $\{X_n\}$

$$AX = B \tag{8}$$

where

$$A_{mn} = \int \underline{g}_m^*(\underline{k}) \cdot [\hat{\underline{Y}}(\underline{k}) + \tilde{\underline{Y}}(\underline{k})] \cdot \underline{g}_n(\underline{k})\, d\underline{k} \tag{9a}$$

$$B_m = \int \underline{g}_m^*(\underline{k}) \cdot \hat{\underline{Y}}_t(\underline{k}) \cdot \underline{V}^i(\underline{k})\, d\underline{k} \tag{9b}$$

A way to construct the set $\{\underline{g}_n(\underline{k})\}$, is to Fourier transform a complete set of functions defined on the aperture. After solving the linear system, eqn. 8, the total voltage $\underline{V}(\underline{k})$ at section $z = 0$ is known, and the scattered voltages on both sides of the structure, at $z = z_l$ and $z = z_r$, can be computed by circuit considerations as:

$$\hat{\underline{V}}^s(\underline{k}) = \hat{\underline{\Gamma}}_c(\underline{k}) \cdot \underline{V}^i(\underline{k}) + \hat{\underline{T}}(\underline{k}) \cdot \underline{V}(\underline{k}) \tag{10a}$$

$$\tilde{\underline{V}}^s(\underline{k}) = \tilde{\underline{T}}(\underline{k}) \cdot \underline{V}(\underline{k}) \tag{10b}$$

where $\hat{\underline{\Gamma}}_c(\underline{k})$ is the dyadic reflection coefficient of the complete structure looking from the left side when the perforated screen is substituted with a solid one. $\hat{\underline{T}}(\underline{k})$ and $\tilde{\underline{T}}(\underline{k})$ are dyadic transmission coefficients of the dielectric layers, relating the scattered voltages to the total voltage at $z = 0$. The expressions of these operators are readily found by transmission line techniques. In particular, in the case of a free-standing screen, $\hat{\underline{\Gamma}}_c(\underline{k}) = -\underline{\mathscr{I}}$ and $\hat{\underline{T}}(\underline{k}) = \tilde{\underline{T}}(\underline{k}) = \underline{\mathscr{I}}$, where $\underline{\mathscr{I}}$ is the unit dyadic.

These equations yield the complete solution of the scattering problem for an arbitrarily perforated metallic screen in a stratified dielectric medium.

We now particularise the results for the case of a periodic arrangement of apertures on a lattice, defined by the basis vectors $\underline{d}_1$, $\underline{d}_2$. To obtain a spectral characterisation of this kind of structure, we assume that the incident field is a plane wave with a transverse wave vector $\underline{K}_t$ and arbitrary polarisation. Under this assumption, the unknown function $\underline{V}(\underline{k})$ can be written as

$$\underline{V}(\underline{k}) = \underline{V}^0(\underline{k}) \sum_{pq} \delta(\underline{k} - \underline{K}_{pq}) \tag{11}$$

where

$$\underline{K}_{pq} = \underline{K}_t + p\underline{K}_1 + q\underline{K}_2 \tag{12}$$

and $\underline{K}_1$, $\underline{K}_2$ are the basis vectors of the reciprocal lattice [5] and $\underline{V}^0(\underline{k})$ is the Fourier transform of the transverse electric field on the central aperture. Eqn. 11 points out that the structure excites a discrete spectrum of plane waves, characterised by transverse wavevector $\underline{K}_{pq}$ (Floquet modes). The unknown of the problem is now $\underline{V}^0(\underline{k})$, and this is the function to be expanded on the set $\{\underline{g}_n(\underline{k})\}$, the inverse Fourier transforms of which, in this case, have support on the central aperture only since, in eqn. 7, we may factor out the same Dirac comb as in eqn. 11. Owing to the fact that the Floquet modes constitute a discrete spectrum, the integrals of eqns. (9a and b) are converted into summations on the indices $p$, $q$:

$$A_{mn} = \sum_{pq} \underline{g}_m^*(\underline{K}_{pq}) \cdot [\hat{\underline{Y}}(\underline{K}_{pq}) + \tilde{\underline{Y}}(\underline{K}_{pq})] \cdot \underline{g}_n(\underline{K}_{pq}) \tag{13a}$$

$$B_m = \sum_{pq} \underline{g}_m^*(\underline{K}_{pq}) \cdot \hat{\underline{Y}}_t(\underline{K}_{pq}) \cdot \underline{V}^i(\underline{K}_{pq}) \tag{13b}$$

Theoretically, eqn. 8 is an infinite system of linear equations, the coefficients of which are expressed as double infinite summations over the points of the reciprocal lattice. To obtain a numerical solution, the number of expansion functions has to be limited to $N_f$ and the number of points of the reciprocal lattice must be truncated to $N_l$. These two truncations are not independent, and can cause convergence problems, as discussed in the following section.

Eqn. 13 can be written more concisely with a matrix formalism. Let us define a $N_l \times N_f$ abstract matrix $Q$ whose element $Q_{mn}$ is the $n$th vector basis function $\underline{g}_n(\underline{k})$ evaluated in the $m$th point of the reciprocal lattice. Notice that the subscript $m$ stands for the couple $(p, q)$ introduced before. Likewise, let us introduce the $(N_l \times N_l)$ abstract diagonal matrices $\hat{Y}$, $\tilde{Y}$ and $\hat{Y}_t$, whose elements are the previously defined dyadic operators $\hat{\underline{Y}}(\underline{k})$, $\tilde{\underline{Y}}(\underline{k})$ and $\hat{\underline{Y}}_t(\underline{k})$ evaluated in the points of the reciprocal lattice. With these definitions, the $(N_f \times N_f)$ system matrix $A$ and the $(N_f)$ column vector $B$, given by eqn. 13, can be rewritten in the compact form

$$A = Q^+[\hat{Y} + \tilde{Y}]Q \tag{14a}$$

$$B = Q^+\hat{Y}_t\hat{V}^i \tag{14b}$$

where $^+$ denotes complex conjugate and transposition. The elements of $A$ and $B$ are scalars, whereas those of the $(N_l)$ column vector $\hat{V}^i$ are two-dimensional vectors since it represents the Fourier transform of the transverse incident electric field at $z = z_l$. This vector represents also the field excited by an adjacent screen with the same lattice, but possibly with apertures of different shape.

Taking into account that eqn. 7 can be written in terms of the projection matrix $Q$ as

$$V = QX \tag{15}$$

the solution of the scattering problem, given by eqn. 10, can now be expressed in matrix form as follows:

$$\hat{V}^s = [\hat{\Gamma}_c + \hat{T}W\hat{Y}_t]\hat{V}^i \tag{16a}$$

$$\tilde{V}^s = \tilde{T}W\hat{Y}_t\hat{V}^i \tag{16b}$$

where

$$W = QA^{-1}Q^+, \tag{17}$$

and $\hat{\Gamma}_c$, $\hat{T}$, $\tilde{T}$ are $(N_l \times N_l)$ abstract diagonal matrices having as elements the dyadic operators $\hat{\underline{\Gamma}}_c(\underline{k})$, $\hat{\underline{T}}(\underline{k})$, $\tilde{\underline{T}}(\underline{k})$ evaluated in the points of the reciprocal lattice.

In order to compute the GSM of the structure, we must consider also the case where a field, with the same discrete spectrum, is incident on the right side ($\tilde{V}^i$). It is easy to see that the solution in this case is obtained by exchanging the superscripts ˆ and ˜ in eqns. 16a and b. Notice that the matrix $W$ is the same in both cases because it depends only on the structure, and not on the excitation. In conclusion, the GSM can be written as

$$\begin{pmatrix} \hat{V}^s \\ \tilde{V}^s \end{pmatrix} = \left( \begin{array}{c|c} \hat{\Gamma}_c + \hat{T}W\hat{Y}_t & \hat{T}W\tilde{Y}_t \\ \tilde{T}W\hat{Y}_t & \tilde{\Gamma}_c + \tilde{T}W\tilde{Y}_t \end{array} \right) \begin{pmatrix} \hat{V}^i \\ \tilde{V}^i \end{pmatrix} \tag{18}$$

The GSM so obtained can be seen as the sum of two terms. The first is the GSM of the structure, where the metallic discontinuity has been substituted with a solid metallic plate ($W = 0$ in eqn. 18). The second takes into account the effect of the apertures, and is related to the radiation of the equivalent magnetic currents placed on a solid metallic plate ($\hat{\Gamma}_c = \tilde{\Gamma}_c = 0$ in eqn. 18).

Once the GSM of each screen in its dielectric environment is known, the GSM of structures constituted by several screens with the same lattice can be derived by standard cascading procedure. To this end, it is convenient to classify the $(2N_l)$ Floquet modes (TE, TM) used to construct the relevant Green function as 'accessible' or 'localised', according to their attenuation in the dielectric layers [21]. The former, either propagating or cutoff, are responsible for the interaction through adjacent discontinuities, while the latter are so attenuated that they do not 'see' the other screens, and give rise only to energy storage if the dielectric are lossless. In cascading the various GSM's, only the accessible mode ports are involved, whereas the localised mode ports can be terminated with the input impedances of the dielectric loads. In this way, multiple screen structures are characterised with great efficiency by reducing to the minimum the size of the matrices to be inverted.

## 3 Results

In this Section, we report on the application of the general formulation that we have described previously to the case of metallic screens periodically perforated with circular apertures of radius $a$. We choose as basis functions $\{g_n(\underline{k})\}$ the Fourier transforms of the mode functions of a circular waveguide of radius $a$. In this way, the basis functions can be expressed in closed form. Although this set does not satisfy the edge condition, the elements of the scattering matrix are computed with adequate accuracy because they are related to variational quantities.

When we use a numerical technique to solve a scattering problem where more than one expansion set is involved, we must address the problem of relative convergence, which arises when the series are truncated to a finite number of terms [22–26]. As is well known, the key point is the correct choice of the ratio between the number of terms retained in the expansions. The criteria based on the conservation of complex power through the discontinuity, on the reciprocity theorem, or on the fact that the fundamental mode equivalent circuit of the screen must be constituted by a purely imaginary shunt admittance [4, 12] are automatically satisfied for any projection $Q$ matrix such that the system matrix $A$ in eqn. 14$a$ is invertible. In other words, these conditions reflect intrinsic properties of the modal formalism, and hence can be exploited only to check the numerical implementation, and not to verify the accuracy of the solution. The correct criterion, although valid only for rectangular lattice and apertures, was given in Reference 11. Recently, the truncation process of the Floquet spectrum has been interpreted as being equivalent to modifying the used basis functions [26]. However, the relative convergence problem can be solved directly in the spectral domain for general geometries, for example circular apertures and triangular lattice, by introducing the concept of spectral bandwidth. In fact, we must recognise that the aperture electric field is represented by means of two sets, that in our case are the inverse Fourier transforms of the basis functions $\{g_n(\underline{k})\}$ and the Floquet modes. To have a well conditioned system matrix $A$, it is important that the accuracies of the two approximations are comparable. In other words, the spectral bandwidths of the two representations must be identical. This criterion gives the number of Floquet modes as a function of the number of basis functions involved. The basis functions chosen have an oscillatory behaviour with a maximum (main lobe) in correspondence of the circular waveguide cutoff wavenumber, and decreasing amplitude beyond it. Therefore, the spectral bandwidth of the representation in terms of basis functions, which in principle is infinite, can be defined in practice so as to include the main lobe of the highest order basis function considered. Fig. 4 shows a plot of the normalised susceptance of a perforated screen

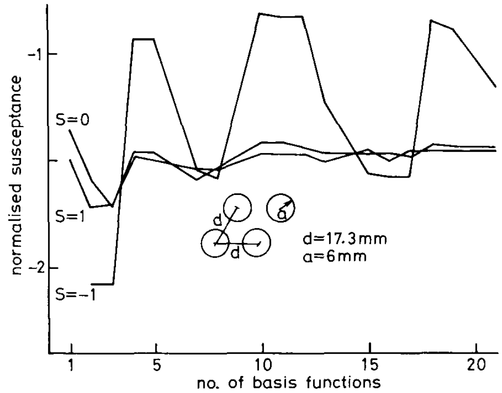


**Fig. 4** *Relative convergence of the numerical solution*
Normalised susceptance of a perforated screen for normal incidence against number of expansion functions for three truncation limits of the Floquet set
$a = 6$ mm $\quad d = 17.3$ mm

for normal incidence at 14 GHz, against the number of basis functions used to represent the aperture field. The curves refer to three different choices for the truncation of the Floquet set. The figure shows that it is important to take into account all the Floquet modes with $|\underline{K}_{pq}|$ up to the main lobe ($s = 0$) of the highest order basis function. Inclusion of more Floquet modes up to the first sidelobe ($s = 1$) does not improve the results in a significant way. Exclusion of the main lobe contribution ($s = -1$) gives rise to large errors because the Floquet modes considered cannot represent the aperture field with the same accuracy as the basis function set.

Perforated screens can be seen as high-pass structures with a frequency response characterised by a reflection band at low frequency, and a transmission band at the resonance frequency. This resonance frequency is very close to the grating lobe limit, and is strongly influenced by the mutual coupling among the apertures. Figs. 5$a$ and $b$ show a normalised plot of the resonance frequency, and of the $-0.5$ dB transmission bandwidth against the geometrical parameters for a free-standing screen (normally illuminated), with the apertures arranged in an equilateral triangular and square lattice, respectively. In the region to the left of the inclined straight line, grating lobes exist.

As is well known, the equivalent circuit for the fundamental mode of a perforated screen is a shunt admittance the value of which depends (apart from the frequency and the geometrical parameters) on the dielectric layers in which the screen is embedded. A suitable dielectric loading can be used to remove the transmission band from the grating lobe limit, if required by the FSS design specifications. As an example of this effect, Fig. 6 shows a plot of the first resonance frequency (zero of the screen admittance) as a function of the dielectric thickness, for several values of the dielectric constant. Since a dielectric layer is present, the zero of the grid admittance does not coincide with the zero of the reflection coefficient. The dependence of the resonance frequency on the dielectric thickness is related to the interaction between the dielectric free-space interface and the screen discontinuity through the higher order Floquet modes. Although the first ones of these modes are propagating in the dielectric, they do not carry active power since they are reactively

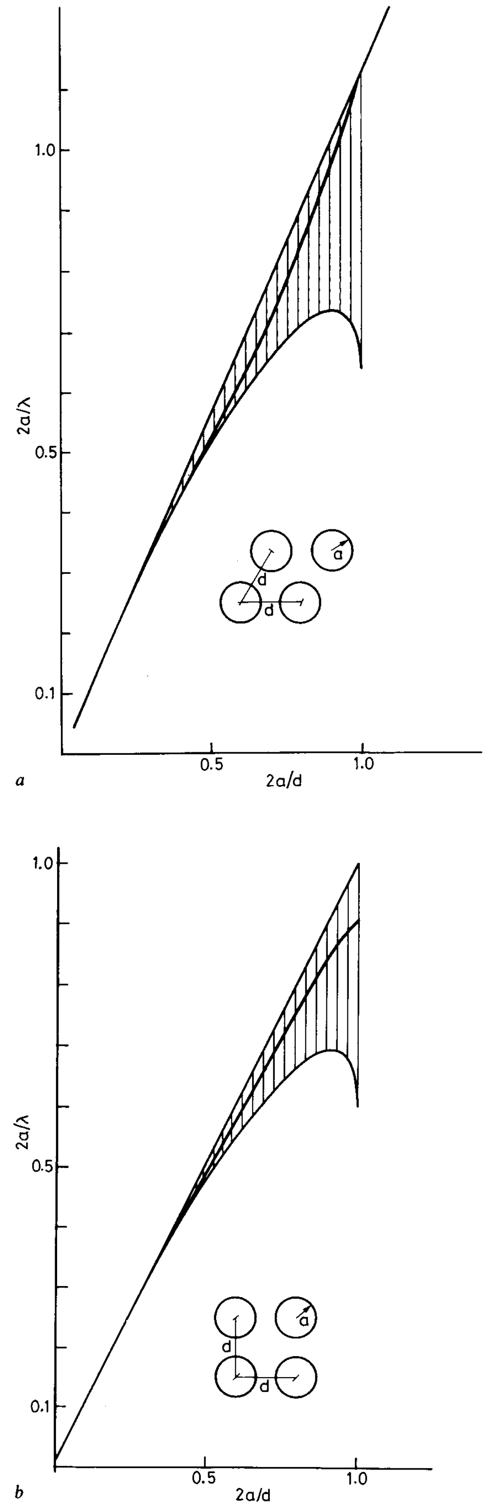


**Fig. 5** *Normalised resonance frequency and −0.5 dB transmission bandwidth of a perforated screen for normal incidence*

*a* Triangular lattice; *b* Square lattice. For $2a/d = 1$ the apertures are tangent hatched region shows transmission bandwidth

loaded. In other words, the screen equivalent circuit is still a pure susceptance even if grating lobes are present in the dielectric.

The transmission bandwidth and the reflection/transmission band spacing ratio of an FSS can be improved if multiple screen structures are used. To point out the essential role played by evanescent mode coupling between adjacent screens, we show the results relative to a couple of identical perforated screens (square lattice, $d = 20$ mm, $a = 8$ mm), spaced 5 mm apart, in two configurations. In the first one (i), the apertures are superimposed, whereas in the second one (ii) there is a half period transversal shift. Fig. 7 shows plots of the reflection and transmission coefficient for normal incidence. As could be expected, the reflection bandwidth in configuration (ii) is larger than in configuration (i), and the opposite happens for the transmission bandwidths. It should be remarked that this behaviour is due to the interaction through the evanescent fields, since it can be proved that, if they are neglected, the frequency response of the complete structure does not depend on the transversal shift of the screens.

It is interesting to note that, in a closely spaced multiple grid configuration, an active power flow is associated to the higher order modes, in the region between the screens only. This phenomenon is reflected in the presence of screen admittances with positive and negative real parts in the equivalent circuit for the fundamental mode. Notice that these admittances are not the equivalent circuits of each screen, but the input admittances of a two-port network, connected in parallel to the fundamental mode transmission line at the sections at which the screens are located. Hence, a reaction loop is established through the evanescent modes. It can be verified numerically that the power dissipated by the first admittance is equal to that generated by the second one, as it is to be expected since the structure is lossless. Fig. 8 shows plots of the screen admittances at $f = 10.2$ GHz against the screen spacing for the same structure previously discussed (configuration *i*). If the spacing is large, the admittances become purely imaginary because the interaction takes place only through the fundamental mode. Moreover, the two imaginary parts asymptotically coincide, because the screens are identical. Conversely, when the spacing vanishes, the two admittances have a sum which is purely imaginary, and tends to the isolated grid value. In this case, all the Floquet modes are accessible.

When perforated screens are used as diplexers, we must analyse their behaviour for oblique incidence. An example is shown in Fig. 9 where the reflection and transmission curves of a 45° incidence diplexer are reported. The structure, sketched in Fig. 10 consists of two identical screens with circular apertures of radius 2.4 mm arranged in an equilateral triangular lattice of size 5 mm. The screens are covered with a 0.05 mm kapton film, and spaced with a 0.6 mm kevlar sheet. The analysis takes into account the fibre structure of these materials, which are characterised by a dyadic dielectric permittivity. In particular, we have assumed a transversal and longitudinal dielectric constants 3.2 and 2.8 for the kapton film, and 4.1 and 3.8 for the kevlar sheet. The curves presented are relative to three different planes of incidence ($\phi = 0°$, 15°, 30°) for TE and TM polarisation. The common −0.5 dB reflection band extends from low frequency up to 9 GHz and, as could be expected, is essentially independent of the plane of incidence. The tight coupling between the screens and the presence of the dielectric supports increases the spacing between the transmission frequency and the grating lobe frequency (40.6 GHz for this incidence). In fact, in this case the common $-0.5$ dB transmission band is located between 24 and 29 GHz. The rather irregular behaviour of the curves above the transmission band is owing to the strong frequency variation of the screen admittances. Notice that the plane at $\phi = 15°$ is not a plane of symmetry of the structure, and mode conversion between TE and TM polarisations occurs. Within the reflection and transmission bands, however, this mode conversion is lower than $-30$ dB. The presence of high polarisation conversion in the transition band is indicated in Fig. 9 by the fact that the transmission and reflection curves for $\phi = 15°$ are not complementary.

The results we have presented have been obtained with a computer code which has been validated with the

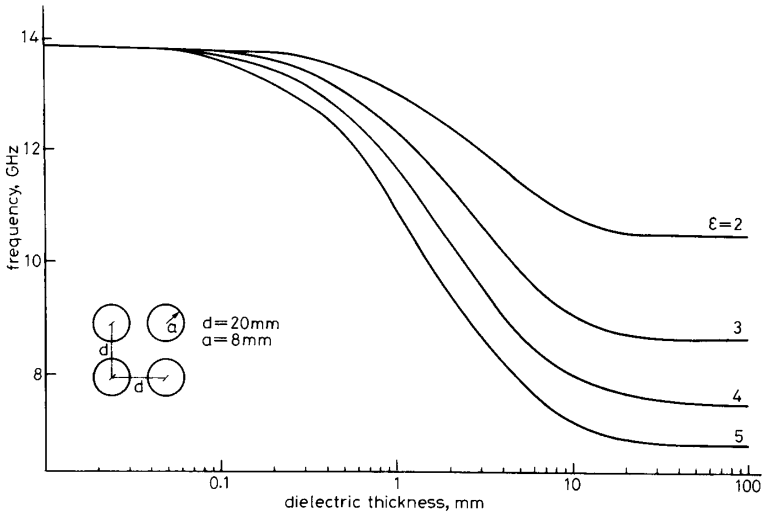


**Fig. 6** *First resonance frequency of a dielectric backed screen against dielectric thickness (normal incidence)*
$a = 8$ mm $d = 20$ mm

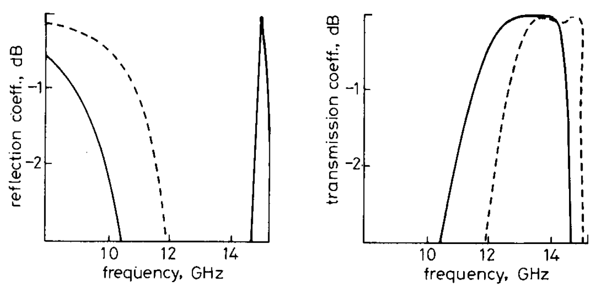


**Fig. 7** *Frequency response of a double screen for normal incidence*
Circular apertures ($a = 8$ mm) in a square lattice ($d = 20$ mm); screen spacing 5 mm
——— no transverse shift between screens
- - - - half-period transverse shift between screens

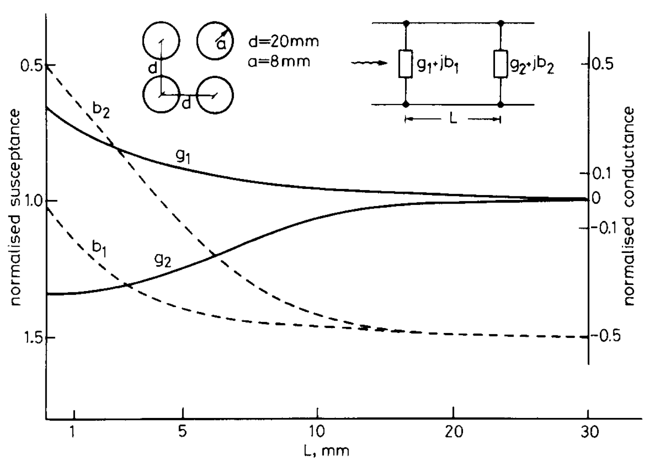


**Fig. 8** *Screen admittances of a double screen structure against screen spacing at normal incidence*
Frequency $f = 10.2$ GHz
$a = 8$ mm $d = 20$ mm

data published in the literature. Moreover, this code has been also validated by analysing a rectangular waveguide iris with circular apertures. As is well known, the iris discontinuity comprises more than one cell, the reflection coefficient for the $TE_{10}$ waveguide mode, and for the $TE_{00}$ Floquet mode, are identical. If the iris contains only

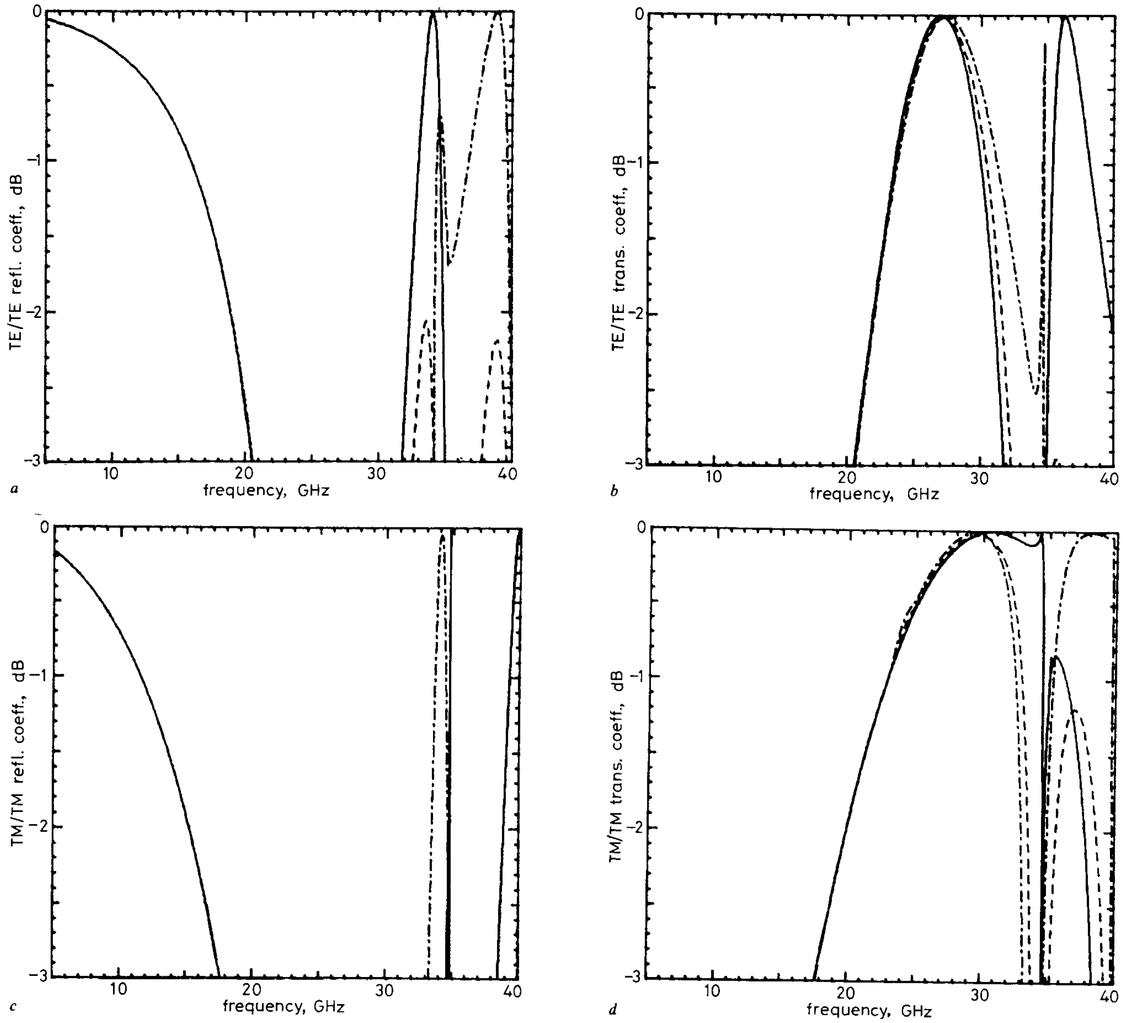


**Fig. 9** *Frequency response for TE and TM polarisations and three planes of incidence of the structure of Fig. 9*
$\theta = 45°$
-·-·- $\phi = 30°$
– – – $\phi = 15°$
—— $\phi = 0°$

one cell, the $TE_{10}$ waveguide mode reflection coefficient is the sum of the reflection coefficient for the fundamental Floquet mode ($TE_{00}$ incident, $TE_{00}$ reflected) and the transreflection coefficient for the first higher order Floquet mode ($TE_{-10}$ incident, $TE_{00}$ reflected). This complication is owing to the fact that in this arrangement the first two TE Floquet modes have opposite transverse wavenumbers and hence are both propagating.

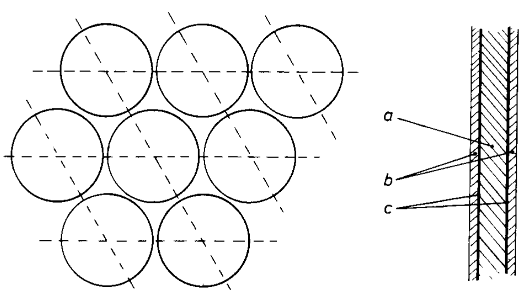


**Fig. 10** *Geometry of the 45° incidence diplexer, front and side view*
*a* 0.6 mm-kevlar sheet, $\varepsilon_t = 4.1$; $\varepsilon_z = 3.8$
*b* 0.05 mm-kapton films, $\varepsilon_t = 3.2$; $\varepsilon_z = 2.8$
*c* screens: $a = 2.4$ mm $d = 5$ mm

equivalent circuit can be derived from the study of a perforated screen with lattice dimensions related to the waveguide dimensions. In particular, if the waveguide

## 4 Conclusions

A spectral vector formulation of the electromagnetic scattering from multiple perforated screens has been presented. The analysis has been carried out for arbitrary perforations, and the results have been specialised to the periodic case. We may observe that it has been relatively easy to derive the functional equation of this problem, even for screens embedded in a general dielectric layered medium, by using the transmission line technique to obtain the relevant Green function. This fact shows the convenience of the spectral approach, with respect to a direct one, in the spatial domain, where the relevant integral equation cannot be obtained so simply when arbitrary stratified dielectrics are present.

As for the numerical solution of the problem, obtained by the Galerkin method of moments, a general truncation criterion has been presented and applied to the case of circular apertures.

The study of multiple screen structures has been carried out in circuit terms by cascading the generalised scattering matrix of each screen in its dielectric environment, exploiting the definition of accessible and localised modes to increase the efficiency. The interaction between closely spaced screens and the effect of a dielectric loading have been discussed in detail, pointing out the consequences on the screen equivalent circuits.

An example of anisotropic kapton and kevlar sheets being used as loading dielectrics has shown the possibility of using perforated screens as diplexers.

Finally, the good agreement between numerical and experimental results for an iris in rectangular waveguide confirms the validity of the approach presented.

## 5 References


1 LANGLEY, R.J., and DRINKWATER, A.J.: 'Improved empirical model for the Jerusalem cross', *IEE Proc. H*, 1982, **129**, p. 146

2 LANGLEY, R.J., and PARKER, E.A.: 'Equivalent circuit model for arrays of square loops', *Elect. Lett.*, 1982, **18**, pp. 294–296

3 LEE, S.W., ZARRILLO, G., and LAW, C.L.: 'Simple formulas for transmission through periodic metal grids or plates', *IEEE Trans. Antennas Propagat.*, 1982, **AP-30**, pp. 904–909

4 COMPTON, R.C., and RUTLEDGE, D.B.: 'Approximation techniques for planar periodic structures', *IEEE Trans. Microwave Theory Tech.*, 1985, **MTT-33**, pp. 1083–1088

5 MONTGOMERY, J.P.: 'Scattering by an infinite periodic array of thin conductors on a dielectric sheet', *IEEE Trans. Antennas and Propagat.*, 1975, **AP-23**, pp. 70–75

6 HAMDY, S.M.A., and PARKER, E.A.: 'Current distribution on elements of a square loop frequency selective surface', *Electron. Lett.*, 1982, **18**, pp. 624–626

7 PARKER, E.A., HAMDY, S.M.A., and LANGLEY, R.J.: 'Modes of resonance of the Jerusalem cross in frequency selective surfaces', *IEE Proc. H*, 1983, **130**, pp. 203–208

8 TSAO, C.H., and MITTRA, R.: 'Spectral domain analysis of frequency selective surfaces comprised of periodic arrays of crossed dipoles and Jerusalem crosses', *IEEE Trans. Antennas and Propagat.*, 1984, **AP-32**, pp. 478–486

9 MITTRA, R., HALL, R.C., and TSAO, C.H.: 'Spectral domain analysis of circular patch frequency selective surfaces', *IEEE Trans. Antennas Propagat.*, 1984, **AP-32**, pp. 533–536

10 ORTA, R., TASCONE, R., and ZICH, R.: 'Frequency selective surfaces: spectral characterization and application to multifrequency antenna systems', *Ann. Telecommun.*, 1985, **40**, (7–8), pp. 378–386

11 LEE, S.W.: 'Scattering by dielectric loaded screen', *IEEE Trans. Antenna Propagat.*, 1971, **AP-19**, pp. 656–665

12 CHEN, C.C.: 'Diffraction of electromagnetic waves by a conducting screen perforated periodically with circular holes', *IEEE Trans. Microwave Theory Tech.*, 1971, **MTT-19**, pp. 475–481

13 CHEN, C.C.: 'Transmission of microwave through perforated flat plates of finite thickness', *IEEE Trans. Microwave Theory Tech.*, 1973, **MTT-21**, (1), pp. 1–6

14 RUBIN, B.J.: 'Scattering from a periodic array of apertures or plates where the conductors have arbitrary shape, thickness and resistivity', *IEEE Trans. Antennas Propagat.*, 1986, **AP-34**, pp. 1356–1365

15 MUNK, B.A., LUEBBERS, R.J., and FULTON, R.D.: 'Transmission through a two-layer array of loaded slots', *IEEE Trans. Antennas Propagat.*, 1974, **AP-22**, pp. 804–809

16 LUEBBERS, R.J., and MUNK, B.A.: 'Mode matching analysis of biplanar slot arrays', *IEEE Trans. Antennas Propagat.*, 1979, **AP-27**, pp. 441–443

17 VARDAXOGLOU, J.C., and PARKER, E.A.: 'Modal analysis of scattering from two-layer frequency-selective surfaces', *Int. J. Electronics*, 1985, **58**, pp. 827–830

18 SHULEY, N.V.: 'Higher-order mode interaction in planar periodic structures', *IEE Proc. H*, 1984, **131**, (3), pp. 129–132

19 JOHANSSON, F.S.: 'Analysis and design of double layer frequency selective surfaces', *IEE Proc. H*, 1985, **132**, (5), pp. 319–325

20 FELSEN, L., and MARCUVITZ, N.: 'Radiation and scattering of waves' (Prentice-Hall, 1973)

21 ROZZI, T.E.: 'Network analysis of strongly coupled transverse apertures in waveguide', *Int. J. Circuit Theory Appl.*, 1973, **1**, pp. 161–178

22 LEE, S.W., JONES, W.R., and CAMPBELL, J.J.: 'Convergence of numerical solutions of iris-type discontinuity problems', *IEEE Trans. Microwave Theory Tech.*, 1971, **MTT-19**, pp. 528–536

23 MITTRA, R., ITOH, T., and LI, T.: 'Analytical and numerical studies of the relative convergence phenomenon arising in the solution of integral equation by the moment method', *IEEE Trans. Microwave Theory Tech.*, 1972, **MTT-20**, pp. 96–104

24 LEROY, M.: 'Convergence of numerical results in modal analysis', *IEEE Trans. Antennas Propagat.*, 1983, **AP-31**, pp. 655–659

25 SHULEY, N.V.: 'Relative convergence for moment method solutions of integral equations of the first kind as applied to dichroic problems', *Electron. Lett.*, 1985, **21**, pp. 95–97

26 JOHANSSON, F.S.: 'Convergence phenomenon in the solution of dichroic scattering problems by Galerkin's method', *IEE Proc. H*, 1987, **130**, pp. 87–92